

Know Your Neighborhood: General and Zero-Shot Capable Binary Function Search Powered by Call Graphlets

Josh Collyer
Loughborough University

Tim Watson
Loughborough University

Iain Phillips
Loughborough University

Abstract

Binary code similarity detection is an important problem with applications in areas like malware analysis, vulnerability research and plagiarism detection. This paper proposes a novel graph neural network architecture combined with a novel graph data representation called call graphlets. A call graphlet encodes the neighborhood around each function in a binary executable, capturing the local and global context through a series of statistical features. A specialized graph neural network model is then designed to operate on this graph representation, learning to map it to a feature vector that encodes semantic code similarities using deep metric learning.

The proposed approach is evaluated across four distinct datasets covering different architectures, compiler toolchains, and optimization levels. Experimental results demonstrate that the combination of call graphlets and the novel graph neural network architecture achieves state-of-the-art performance compared to baseline techniques across cross-architecture, mono-architecture and zero shot tasks. In addition, our proposed approach also performs well when evaluated against an out-of-domain function inlining task. Overall, the work provides a general and effective graph neural network-based solution for conducting binary code similarity detection.

1 Introduction

Binary code similarity detection (BCSD) aims to find compiled functions that are similar to a given query function. It has a wide range of applications, from identifying vulnerabilities in firmware to analyzing code reuse across malware variants. BCSD can enhance security assessments of closed-source software by accurately identifying the components used, such as libraries embedded within statically linked executables and firmware binaries.

Implementing effective BCSD approaches is challenging due to the diversity of architectures, compiler toolchains, and optimization levels used to build software. These factors can lead to significant variations in the binary representations of

the same source code, making it challenging to distinguish between similar and dissimilar functions. While optimization level has the biggest impact on these variations, recent research shows that call graph features are most resilient to these transformations, presenting an opportunity to develop improved, general BCSD approaches [10].

Existing approaches predominantly focus on function-level artifacts like control flow graphs, disassembly, or intermediate representations, neglecting the potential of call graph features. Additionally, some approaches rely on the assumption of dynamically linked standard library functions such as those from *libc* are easily recoverable, which does not hold for embedded devices and malware where static linking is common, restricting their applicability across different software ecosystems.

Furthermore, the evaluation methodologies employed in binary function search often lack rigor. Existing approaches predominantly rely on "in-domain" evaluation data, utilizing subsets of functions from the training binaries themselves. This practice introduces the risk of data leakage, potentially inflating reported performance metrics. More crucially, it fails to assess the true generalization capability of the approach when faced with previously unseen functions, a scenario referred to as "out-of-domain" data. Comprehensive evaluation necessitates testing on entirely separate datasets to obtain an accurate understanding of real-world performance and generalizability. This is an area we tackle head on with evaluation across four distinct datasets.

This paper proposes a novel approach that aims to exploit the additional information available when including call graph features and addresses the limitations of existing methods. It employs a comprehensive evaluation methodology, including both in-domain and out-of-domain assessments across four large datasets, to ensure robust and generalizable findings. The proposed approach does not rely on the identification of standard library functionality, making it applicable across a broader range of binary types and scenarios.

1.1 Key Contributions

Within this work, we propose a general function search approach utilizing function level call graphlets inspired by the results presented in TikNib [10] and PSS [2]. Our contributions are as follows:

1. We introduce a novel call graph level function format we name call graphlets. This format incorporates a functions callers as well as callees to provide a graphlet neighborhood which provides structure alongside a set of simple function level features as node attributes.
2. We present a simple, yet powerful Graph Neural Network (GNN) trained using deep metric learning which is capable performing well in and out of domain across a number of tasks.
3. We present a robust evaluation using previous research datasets of our approach as well as compare against a range of benchmarks.
4. We present conduct an ablation study to investigate how our graph neural network (GNN) design choices contribute to our performance.

1.2 Paper Overview

The remainder of this paper is organized as follows: We begin by reviewing the relevant prior work to establish a foundation for our contributions. Next, we present a detailed description of the methodology used in this study. This includes explaining how a call graphlet is constructed, the features used for nodes and edges, the Graph Neural Network (GNN) architectural choices, and the datasets employed. Following this, we present a comprehensive section on the experiments conducted to evaluate our approach. We start with an evaluation in a cross-architecture context, followed by experiments on the model’s performance in a mono-architecture setting (x86-64 only), cross-architecture with function inlining setting, zero-shot vulnerability search setting, and then conclude with an ablation study. Finally, we conclude the paper by exploring some fundamental limitations of our approaches and providing our concluding remarks.

2 Related Work

The problem of identifying similar functions across different binary architectures has been tackled using various methods in the existing literature. These methods can generally be classified into three main categories: sequence-based approaches and graph-based approaches, or a combination of both. In this section, we start by briefly reviewing the sequence-based approaches. Then, we provide a more detailed review of the graph-based literature. Finally, we will discuss alternative

methods and highlight the limitations of previous works in this area.

2.1 Sequence Based Approaches

Sequence based approaches use either assembly, pseudo-code or intermediate representations extracted from binaries for each function to generate representations suitable for comparison. These sorts of approaches have been applied to individual assembly instructions [13], sequences of assembly instructions [23], sequences of intermediate representations [4] and even execution sequences [18].

All approaches share the common objective of seeking to learn useful representations of input by adapting approaches developed in the natural language processing (NLP) literature. This is typically done via a two stage process of pre-training and then fine-tuning. Researchers have used a range of different pre-training tasks ranging from standard approaches such as Masked Language Modelling (MLM) to domain specific tasks such as jump target prediction [23] and instruction data flow relationship prediction [13]. Once pre-trained, the models are then fine-tuned for a given down stream task such as binary code similarity detection (BCSD) or N-day vulnerability detection typically using contrastive methods such as deep metric learning.

2.2 Graph Based Approaches

All of these approaches however miss an opportunity to use broader information related to a single function such as type information and calling relationships and instead focus on data contained within the a single function boundary. Graph based approaches on the other hand, look to exploit the inherent data structure within compiled binaries such as call graphs and control flow graphs (CFG). These data structures are then paired with graph neural network approaches to create learnt representations that perform well at downstream tasks such as BCSD.

XBA [11] is a graph neural networks approach which works on a basic block level for a given function as well as incorporating key external information such as string literals and external function calls. This novel representation is then fed into a GCN based GNN to generate cross-architecture and cross-platform embeddings. PDM [17] is another example of a graph neural network which instead works on a combined control flow and data flow representation named *ACFG+*. This representation is then used alongside a Capsule GNN to generate embeddings.

CFG2VEC [25] is an example of a more complicated approach to ours and was used as inspiration for our approach. CFG2VEC is a hierarchical method whereby a single input is a binaries entire call graph and each node is a P-code Based control flow graph. The P-Code based CFG representation is then fed into a graph neural network to create

node-embeddings for the higher level call graph. These node embeddings are then subsequently used to support binary code similarity detection tasks. PSS [2] propose an interesting graph spectra approach which operates primarily on the call graphs structure. This approach is used for whole binary identification so can be considered tangential to the other papers within this section but has been included primarily because it was also a large the main inspiration for this work. HermesSim [8] also used a P-Code representation of a target function but instead creates a novel graph representation where nodes are P-code operations or memory locations and the edges are relationships such as read and writes. This is again fed into a GNN approach to create function level representations that can be used for BCSD tasks. HermesSim can be considered the current state of the art in this area having reported impressive results recently.

2.3 Alternative Methods

In addition to sequence, graph and combinatorial methods, some researchers have sort to adopt alternative methods. Bin-Finder [19] is an example of this were instead of using sequences, a series of statistical count features were used based on a VEX IR lifted representation and counts of *glibc* calls. This approach has one major drawback and that is the reliance on *glibc* functions being recoverable and external. This has potential to limit its usage in cases such as statically linked binaries or blob firmware. The approach however does perform very well and is one our a key baselines.

2.4 Limitations of Previous Work

There are several limitations of the works mentioned above. Firstly, several of the approaches [11, 19] rely on recoverable function names to build fundamental parts of there feature space. This is error-prone and something that may not always be possible in all settings such as when you are faced with obfuscated or statically linked binaries. Secondly, most existing approaches [4, 13, 17, 18, 23] analyze individual functions in isolation without considering the broader relationships and interactions between functions within the software binary. This potentially overlooks valuable information that is inherent in the overall structure and interconnections present in the binary.

Thirdly, when approaches utilize external information like global call graphs [2, 25], they encounter two primary limitations. First, a global call graph is a coarse representation, and its structure, and consequently its effectiveness, can be significantly affected by obfuscation techniques and function inlining. Secondly, errors in accurately recovering the correct calling relationships may propagate throughout the entire graph, even though these errors may only impact a subset of the functions within the binary executable, the effect may still be significant.

3 Methodology

3.1 Call Graphlet Neighborhoods

Our work utilizes a novel data format we call *call graphlets* (visually depicted Figure 1). This approach was inspired by the work described in PSS [2] but instead of operating with binary level call graphs, we opt to work with function level ones. A call graphlet is a weighted directed graph made up of a tuple $G = V, E, W$ whereby: V represents a set of functions, E represents a set of calling relationship in the format of $(x, y) \mid x \neq y$ and W represent the weights for a given edge. A target function’s call graphlet neighborhood includes a node for the target function itself, any functions that call the target function (callers), any functions the target function calls (callees) and any functions that are called by the target functions callees (callees of callees). We excluded callers of callers from our call graphlets to prevent creating excessively large call graphlets, particularly for widely used functions like utilities and standard libraries, and because we felt that callee relationships better characterize a function. The weights for all edges correspond to there respective edge betweenness value that is calculated at a call graphlet level rather than a global call graph level.

The reasons for working at a call graphlet level are twofold. Firstly, recent work suggests that features derived from the call graph are the most robust to changes in compilation toolchains [10]. We however viewed using global call graphs as too coarse and instead formulated a more fine grained data representation with the aim of developing a high performing function-level BCSD approach. Secondly, we wanted to create a data representation that took the calling behaviour between a function, its callers and callees into account. We view this relationship as something that will likely be similar within software compiled from the same source code regardless of compilation variations. This provides a means to focus on a higher level representation rather than solely focusing on function level differences or changes such as patches or refactoring.

3.2 Graph Features

3.2.1 Node Features

Each of the functions within a given call graphlet neighborhood have the six straightforward features derived from function level metadata recovered during the disassembly process. Features such as in-degree (number of callers), out-degree (number of callees) and total number of edges provide global information whilst features such as total number of instructions, number of arguments and number of local variables provide local information. The hypothesis is that this combination of local and global level information provides the model the ability to discern between a range of different functions. For example, a complex function that is infrequently

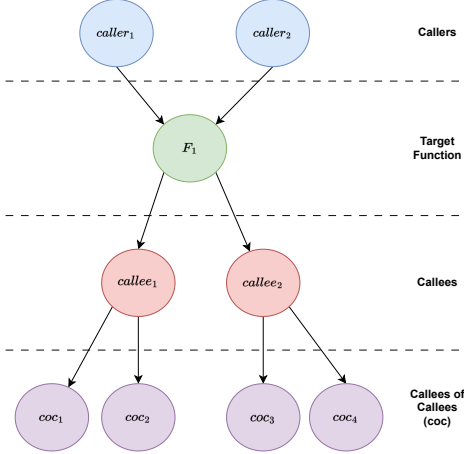


Figure 1: Call Graphlet Example Data Structure

called may have a low in-degree but a high number of instructions, out-degree and number of local variables whereas a wrapper function for a commonly used library function such as *memcpy* may have a low instruction count and out-degree but a very high in-degree suggesting it is called frequently. The full feature list can be found in [Table 1](#).

Feature Name	Description
Num Instructions	The number of instruction in the function
Num Edges	The sum of in-degree and out-degree edges
Total Indegree	The number of in-degree edges. Denotes callers
Total Outdegree	The number of out-degree edges. Denotes callees
Num Locals	The number of local variables
Num Args	Number of arguments from the recovered function prototype

Table 1: Function/Node Level Features

3.2.2 Edge Weights

Alongside the node-level function metadata, we also generate a weight for each edge within the call graphlet using edge betweenness centrality.

The edge betweenness for edge e is calculated as follows:

$$C_b(e) = \sum_{s,t \in V} \frac{\sigma(s,t|e)}{\sigma(s,t)} \quad (1)$$

where V is the set of nodes, $\sigma(s,t)$ is the number of shortest paths between the nodes s and t and $\sigma(s,t|e)$ is the number of shortest paths that pass through e .

The edge betweenness is calculated at a call graphlet level instead of a global call graph level because we want to quantify the control each edge exerts over information flow within the call graphlet. Edges with high betweenness centrality can be viewed as critical pathways or bottlenecks. In our particular case, we viewed edge betweenness centrality as a useful addition because it provides a means of identifying functions that exhibit high call fan-out (i.e., a large number of callees) and participate in critical calling relationships with ancestor functions in the call hierarchy. This additional information is hypothesized to improve the model’s performance by capturing the interplay between a function’s calling behavior and its position within the program’s overall call structure.

3.3 Datasets

3.3.1 Training Dataset

The training dataset used within this paper is the *Dataset-1* released as part of the work of [15]. This dataset contains seven popular open source projects: ClamAV, Curl, Nmap, Openssl, Unrar, z3 and zlib. Each of these are compiled for ARM32, ARM64, MIPS32, MIPS64, x86 and x86-64 using 4 different versions of Clang and GCC alongside 5 different optimization levels. Each project has 24 unique configurations. The same sized train, test and validation splits were created as described in [15] and [8] to support robust comparison.

It is worth noting that the processed call-graphlet dataset created from *Dataset-1* using *bin2ml* is significantly larger than what is reported in [15] and [8]. This is because our data representation allows us to relax the filtering requirements such as number of instruction or basic blocks within a function. Since our method uses a functions neighborhood, we can include smaller functions as they will be augmented by their neighbors who may not fit the filtering requirements.

Our data representation also likely results in more varied examples of each function because, due to architectural, compiler or optimization differences, the variations present within a functions neighborhood are included as well. This is especially interesting because even when the node features of a function are duplicates, each call graphlet may be different and therefore, continue to be included within our dataset. With this being said, in order to facilitate robust and fair comparison, we firstly subset the data into the same binary-level splits described in [15] and then use random sampling to create identically sized samples from within the binaries within the split. This methodology is replicated to generate the corresponding *Dataset-1* test set split as well.

3.3.2 Evaluation Datasets

In order to robustly evaluate our approach, we use four open source benchmark datasets and focus exclusively on out-of-domain evaluation. The reason for focusing exclusively on out-of-domain performance is that it provides experimental

evidence of our approaches performs well when given a collection of binaries it has not already seen as well as being the most comparable to a real-world setting.

Firstly, we use the test set from Dataset-1. This dataset includes a subset binaries which encompasses the Z3 and Nmap projects, all of which are not present within the train dataset. This dataset contains 522003 functions which is identical to the size used within [8] and [15].

Secondly, we use *Dataset-2* also presented in [15]. This dataset is a subset of the evaluation dataset used within [18] and ensures there is no intersection between the software packages contained within *Dataset-1*. *Dataset-2* includes the following 10 libraries: Binutils, coreutils, diffutils, findutils, GMP, ImageMagick, Libmicrohttpd, LibTomCrypt, PuTTY and SQLite. Due to issues processing *ar* archives with our data processing tool, Libmicrohttpd and LibTomCrypt were omitted from our evaluation dataset. Both of these binaries are however included within the later datasets. The binaries within this dataset include versions compiled for x86, x64, ARM32, ARM64, MIPS32 and MIPS64 across four optimization levels (O0, O1, O2, O3) using the GCC-7.5 compiler. This dataset shares the same overall configuration in terms of architectures, optimization levels and compiler version but has unique binaries within it.

Thirdly, we use *BinKit NoInline* dataset presented within [10]. This dataset contains 51 unique packages/libraries across 8 architectures (x86, x64, ARM32, ARM64, MIPS32, MIPS64, MIPS32EB and MIPS64EB), 9 different versions of compiler (five unique versions of GCC, four unique versions of Clang) as well as five different optimization levels (O0, O1, O2, O3, Os). All of the binaries have also been compiled with function inlining turned off. This results in a total of 67,680 binaries. This dataset does share some common software projects to *Dataset-2* but does not share any with the training dataset. This dataset introduces two previously unseen architecture variants, additional compilers as well as an additional optimization level.

And finally, we use the *BinKit Normal* dataset also presented within [10]. This is an identical dataset to the *BinKit NoInline* dataset described above but with one fundamental difference - The compilers are able to inline functions. Function inlining has been referenced as a significant weakness across a number of binary function similarity approaches [6, 24] and therefore this dataset allows us to tackle this area head on and generate empirical results of how well our approach fairs when faced with function inlining.

3.3.3 Data Preparation

A uniform data preparation pipeline was implemented to process all datasets outlined above. This process can be broken down into five key stages: extraction, fusion, deduplication, augmentation and sub-setting.

Extraction: The initial stage involved extracting call graphs and function metadata for each binary within the datasets. This was achieved by utilizing the *bin2ml* tool which uses *radare2* as the underlying software reverse engineering tool to load, process and output the required data.

Fusion: Following extraction, the extracted call graph and function metadata were combined. This process resulted in the creation of function-level call graphlets. Each call graphlet encapsulated the functions local call graph structure whereby each node’s features was it’s corresponding function’s meta-data. Each call graphlet was output as a *Networkx* [7] compatible JSON object to support seamless loading into our chosen graph neural network framework, *PyTorch Geometric* [5].

Deduplication: The next stage focused on eliminating redundant call graphlets within the datasets. The methodology employed here was inspired by previous related work [4, 8, 15]. The deduplication process is outlined as follows:

1. Call graphlets are initially grouped based on the software binary from which they originated. This binary-specific grouping facilitates a more efficient deduplication process.
2. Subsequently, each call graphlet within a group is hashed using a suitable hashing algorithm. The resulting hash values are then stored within a hash set. This hash set serves as a mechanism to track unique call graphlets encountered for each binary.
3. In the event that a duplicate hash is identified, the call graphlet is removed from the dataset. This ensures the presence of a single example for each unique call graphlet.

All of the remaining, unique call graphlets are saved and form the basis of the given dataset used to train or evaluate our proposed approach.

Augmentation: Once deduplication was complete, each graph was loaded into *Networkx* and the edge betweenness values were generated and then appended to the graph as floating point edge weights.

Subsetting: The last stage focused on sub-setting the data. This was not necessary for all datasets but in the case of *BinKit Normal* and *BinKitNoInline*, due to the number of unique functions call graphlets generated, it was not feasible to evaluate a model on all functions present due to hardware limitations. For both, we used a random sampling strategy to create test datasets. Each sample contained a total of 1 million functions. This subset was created once for each source dataset and then saved for re-use. Both of these splits are provided as part of the release of this research.

3.4 Model

The model used within our approach is a bespoke 3-layer graph neural network incorporating several different GNN

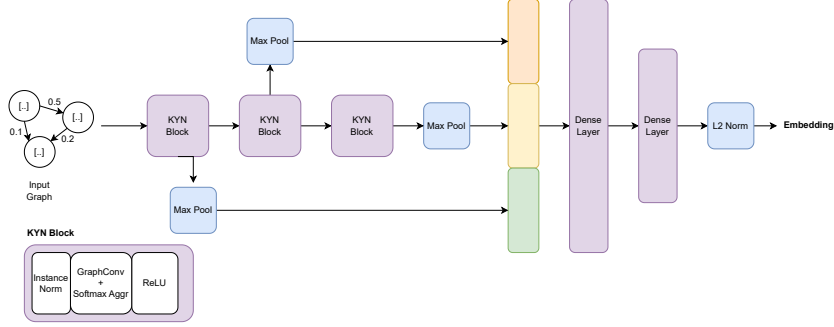


Figure 2: KYN Model Architecture

components to create a novel GNN architecture. A diagram visually representing the model can be seen in [Figure 2](#) **GraphConv Message Passing GNN**

The graph convolution operator used within this study is the operator proposed in [16]. It computes the updated feature representation x'_i for a node i in a graph by combining two components: 1) a linear transformation of the node’s own input features W_1x_i , and 2) a weighted sum of the features of its neighboring nodes $\sum_{j \in N(i)} e_{j,i} \cdot x_j$, where the neighbors’ features are first weighted by the strength of their connections $e_{j,i}$ and then linearly transformed W_2 . The resulting output feature vector x'_i captures both the node’s intrinsic features and the information from its local neighborhood. This operator has been shown to be able to capture higher-order graph structures and outperform a range of standard GNN and graph kernel approaches. This is due to approach considering structures within the graphs at varying scales.

$$x'_i = W_1x_i + W_2 \sum_{j \in N(i)} e_{j,i} \cdot x_j \quad (2)$$

Instance Normalization

We adopt Instance Normalization (IN) [22] as the graph normalization technique omitting the learnable scale and shift parameters γ and β , as described in [Equation 3](#). IN is applied to the node features, where x'_i represents the normalized node feature for node i . It centers the features by subtracting the mean $E[x]$ across all nodes within a given graph, scales them by dividing by the square root of the variance $Var[x]$ plus a small constant ϵ (set to $1e - 05$). This normalization technique aims to stabilize the training process by reducing the internal covariate shift, ensuring consistent distribution of node features across the layers of the graph neural network.

$$x'_i = \frac{x - E[x]}{\sqrt{Var[x] + \epsilon}} \quad (3)$$

Due to the cross-architecture context of our research, the selection of architecture, compiler, and optimization combinations can significantly influence a function’s structure and form. IN exhibits an interesting property wherein it performs

normalization on each function independently at the graph level. This means that variations among features within our examples are handled separately, which is crucial in our domain due to substantial variations across multiple features, such as the number of instructions, total number of edges, in-degree, and out-degree.

Softmax Aggregation

Similar to other recent works such as HermesSim [8], we opt use the Softmax aggregation function as defined as follows:

$$softmax(X|t) = \sum_{x_i \in X} \frac{exp(t \cdot x_i)}{\sum_{x_j \in X} exp(t \cdot x_j)} \cdot x_i \quad (4)$$

where t controls the softness of the softmax aggregation over the input feature set X , which in our case is set to 1. This differs from the usage within HermesSim in two key ways. Firstly, we adopt the vanilla version of softmax aggregation which omits the multi-headed attention extensions. And secondly, we use the softmax aggregation function as the GNN’s aggregation function as opposed to using it as a global graph pooling operator. The softmax operator is used to create node-level representations at each message passing step.

Layer-Wise Connections + Max Pool

We opt to have Layer-Wise feature connections from each of the graph neural network layers to store the node level representations from each convolution. The node-level representations are stored from each layer-wise connection before each of them being max pooled to create a graph level representation where the resulting feature vector is a feature-wise maximum across the node features of that layer. This operation can be seen in [Equation 5](#).

$$X_i = \max_{n=1}^{N_i} X_n \quad (5)$$

Global max pooling was chosen to provide a means of identifying the most distinct features from across the call graphlet node representations. This was viewed favorably given our objective is to identify similar functions across architectures,

compilers and optimization levels which requires distinct representations.

Mapping to Embedding

Each of the max pooled graph-level embeddings are then concatenated together $X_c = (X_1, X_2, X_3)$ resulting in a single vector of size $3 * X_{input}$. This feature vector is then passed into a two layer linear network, mapping from $3 * hidden_d \rightarrow hidden_d \rightarrow \frac{hidden_d}{2}$. The output of this is then normalized using $F2$ normalization to produce the final embedding.

3.5 Training

The model was trained using pair-based deep metric learning using a BatchHard mining scheme [9]. We paid special attention to the sampling methodology to ensure that each batch contained multiple (2 in our case) versions of any function present. This ensured that it was always possible to create a positive pair for each function present as well as provide a rich range of possible negative samples.

The model’s configuration was a hidden dimension size of 256 and an output embedding dimension of 128. Circle loss [21] was used as the loss function configured with m set to 0.25 and γ set to 256. Circle loss and the hyper parameters were chosen due to good results presented in previous works [4]. The model was optimized using the Adam optimizer [12]. The model was trained for 350 epochs with each epoch having 100K graphs randomly sampled from the total training dataset. A cosine simulated annealing with warm restarts learning rate schedule starting at 0.0005 and finishing at 0.0001 was used and each batch had 256 graphs within it. The number of epochs before warm restart started at 50 and doubled for 2 subsequent times (50 -> 100 -> 200) for a total of 350 training epochs.

4 Evaluation

We implement *KYN* using PyTorch Geometric [5]. We use *bin2ml* alongside *radare2* to generate the data for all the experiments outlined below. All experimentation was conducted on a workstation with 64GB RAM alongside a NVIDIA 4090 24GB GPU.

We conducted several in-depth experiments to answer the following research questions:

1. **RQ1:** How does *KYN* perform when faced with unseen libraries, compilers and compiler options in a cross-architecture setting?
2. **RQ2:** How does *KYN* perform when faced with unseen libraries, compilers and compiler options in a mono-architecture setting?
3. **RQ3:** How does *KYN* perform when faced with function inlining when this is not present in the training data?

4. **RQ4:** Is *KYN* capable of performing zero-shot architecture search?
5. **RQ5:** What aspects of the *KYN* model contribute to it’s overall performance?

4.1 Tasks

The evaluation tasks have been formulated to provide a means of holistically evaluating the performance of *KYN* over a large collection of binaries drawn from several benchmark datasets.

For *RQ1*, *RQ2* and *RQ3* we adopt the same approach described in [15] by creating search pools of N size whereby for a given function f , the generated search pool includes a single positive and $N - 1$ negatives. Due to reporting both cross-architecture and mono-architecture results, we have two key subtasks:

1. For cross-architecture datasets, we report results for the *XM* task described in [15]. The *XM* task imposes no restrictions on what architecture, bitness, compiler or optimization level can be chosen and can be considered representative of real life.
2. For mono-architecture datasets (which are all x86-64), we report results comparable to the *XC* task described in [15]. The *XC* task imposes restrictions on the architecture and bitness that can be chosen but no restrictions on compiler or optimization level.

For both cross and mono-architecture evaluation, we provide results across a range of search pool sizes ranging from 100 to 10000. The search pool size of 100 and 10000 are used to compare against other SOTA approaches with the remaining provided for future researchers to compare against.

For *RQ4*, we adopt the vulnerability search task described in [15] with an addition of compiling the same version of *libcrypto.so* for RISC-V 32-bit and PowerPC 32-bit. And finally for *RQ5*, we evaluate the architecture choice impact using the *XM* tasks described above.

4.2 Metrics

To facilitate robust comparison, we adopt the same metrics used within the domain of Recall at 1 ($R@1$) and Mean Reciprocal Rank at 10 ($MRR@10$) [15]. These metrics are used for all results presented as part of *RQ1*, *RQ2* and *RQ3*. At points throughout reporting the results for *RQ1*, *RQ2* and *RQ3* we also report Normalized Discount Cumulative Gain at 10 ($NDCG@10$). $NDCG$ is an alternative metric to MRR and unlike MRR , considered results throughout the K selected rather than just the first occurrence. The $NDCG@10$ scores have been provided to aid future researchers compare against our approach. For *RQ4*, we report the ranks at which the vulnerable function was present at after the search was conducted.

Approach	Summary	100		10,000	
		R@1	MRR@10	R@1	MRR@10
Trex [18]	Disasm + Traces	0.24	0.34	0.09	0.11
GMN [14]	CFG + BoW opc 200	0.45	0.54	0.11	0.16
FASER NRM [4]	ESIL IR Strings	0.51	0.57	-	-
GraphMoco [20]	ASM Basic Block + GNN	0.55	0.60	-	-
BinFinder [19]	VEX IR + Metadata	0.73	0.80	-	-
HermesSim [8]	PCode SOG	0.75	0.80	0.44	0.51
KYN (Ours)	Call Graphlets + Metadata	0.76	0.80	0.45	0.50

Table 2: Dataset-1 (Cisco Talos Binary Similarity [15]) Test Results across search pools of 100 and 10,000 compared against relevant benchmarks

This is the same as previous studies [15]. We also report the mean and median rank to support comparison in a similar manner to [4].

4.3 Baseline Approaches

In order to robustly evaluate our approach, we have chosen a range of state-of-the-art baselines approaches which include both graph and sequence based models.

1. **Trex** [18] is a transformer model trained on both disassembly and micro traces in order to learn execution semantics before then being fine-tuned for the binary function search task.
2. **GMN** [14] is a variant of the GNN proposed in the same paper and have been shown to outperform alternative baseline graph neural network approaches [15]. This approach does however rely on 1-to-1 matching across the entire comparison corpus which is a significant drawback.
3. **FASER** [4] is cross-architecture binary code similarity detection approach that combines long context transformers with radare2’s native intermediate representation.
4. **GraphMoco** [20] is a hybrid model which first encoded basic blocks before then generating embedding representations with a GNN.
5. **Binfinder** [19] is a simple feed-forward neural network which leverages VEX IR and several statistical features to identify similar features.
6. **HermesSim** [8] is a state of the art approach that leverages a novel graph data structure named *Semantic Orientated Graph* alongside a graph neural network to embed functions before then comparing them.

For the mono-architecture experiments, we also compare against **jTrans** [23]. jTrans is a transformer model trained

using a novel jump orientated pre-training task on a large x86-64 dataset and can be considered as one of the state of the art models for x86-64 mono-architecture binary function search.

4.4 Cross Architecture Binary Function Search (RQ1)

4.4.1 Dataset 1

The results presented in the Table 2 show the results generated for search pools 100 and 10000. Starting first with the results for the smaller, 100 negative search pool size, our approaches performs comparably to the current state of the art approaches, HermesSim [8] and BinFinder [19] with reported metrics that are near identical. When comparing against our other chosen SOTA GNN baselines, GraphMoco [20] and GMN [14], our approach significantly outperforms across all collected metrics with a R@1 relative increase of 32% and 51.2% and a MRR@10 relative increase of 28.6% and 38.8% respectively. When compared against two state of the art cross-architecture Transformer models FASER [4] and Trex [18], our approach again significantly outperforms them with a R@1 relative increase of 39.8% and 104% and a MRR@10 relative increase of 33.6% and 80.7%. Turning now to the larger search pool size of 10000, our proposed approach again reports near identical results to HermesSim with a marginally better R@1 but a lower MRR@10 suggesting both approaches are performing similarly.

In addition to the search pools sizes of 100 and 10,000, we also present results for the search pool sizes of 250 and 1000 in Table 3. This was primarily due to how significant the difference is for the results between 100 and 10,000 is and provides a means of reasoning about the performance degradation as the pool size increases as well as providing future researchers empirical results to compare against.

The results presented in Table 3 show that, as expected, all metrics degrade as the search pool size increases, with the degradation occurring steadily. Notably however, our ap-

Approach	Summary	XA + XO	
		R@1	MRR@10
Trex	512 Tokens	0.46	0.53
GNN (from authors of GMN)	CFG + BoW opc 200	0.57	0.67
GMN	CFG + BoW opc 200	0.61	0.71
KYN (Ours)	Call Graphlets	0.76	0.82

Table 3: Dataset-2 Test Results across search pools of 100 compared against relevant benchmarks. Comparison scores taken directly from [15]

proach even outperforms the bottom four baselines (Trex, GMN, FASER, GraphMoco) when faced with search pools containing 1,000 functions compared to when each of the approaches is dealing with only 100 functions. This demonstrates the effectiveness of our approach, especially when faced with a larger number of possible candidate functions to search.

4.4.2 Dataset-2

The results shown Table 4 demonstrate that our approach significantly outperforms all the baseline approaches. Compared to the best baseline, our method achieves a 22.9% increase in R@1 (recall at 1) and a 14.8% increase in MRR@10 (mean reciprocal rank at 10). Interestingly, the performance of our approach is comparable to the results we obtained for Dataset-1. This is not the case for the baseline approaches, which perform better on this dataset than on Dataset-1. This suggests that not only does our model outperform the baselines in terms of the metric scores, but it also exhibits more consistent performance across different datasets.

Search Pool Size	R@1	MRR@10	NDCG@10
250	0.670	0.711	0.735
1000	0.572	0.616	0.641

Table 4: Results for Dataset-1 Across Different Search Pools

In a similar manner to Dataset-1, we also generated results for search pools of 250, 1000 and 10,000. The results for this are presented in Table 5. As the search pool size increases, the performance degradation is more significant. From theorising why this may be, we think this is likely due to the composition of the Dataset-1 test set. The test set split is dominated by the Z3 (in terms of on-disk size and number of functions) resulting in an intrinsically varied sample. When faced with a dataset with more scope for similar functions from different binaries and when at large pool sizes, the task becomes more challenging therefore reducing overall performance.

Search Pool Size	R@1	MRR@10	NDCG@10
250	0.674	0.737	0.765
1000	0.566	0.641	0.679
10000	0.328	0.417	0.461

Table 5: Results for Dataset-2 Across Different Search Pools

4.4.3 Binkit Noinline

The results from evaluating our approach for *binkit-noinline* architecture presented in Table 6. Our approach again performs consistently across all of the metrics collected and reports similar results to those collected when using *Dataset-1* and *Dataset-2*.

Search Pool Size	R@1	MRR@10	NDCG@10
100	0.824	0.873	0.893
250	0.774	0.831	0.858
1000	0.636	0.714	0.751
10000	0.436	0.529	0.574

Table 6: Binkit-Noinline Metrics Across Different Search Pools

4.4.4 Summary

In summary, the results above demonstrate that, after robust evaluation across a range of different binary benchmark datasets, that our approach performs equally or significantly better to comparison benchmarks. The breadth of datasets used for evaluation demonstrates that our approach could be considered a general approach which can generalize to unseen binaries within a cross-architecture setting.

4.5 Mono-Architecture Binary Function Search (x86-64) (RQ2)

Turning now to our mono-architecture evaluation. For this, we use two distinct KYN models, one trained in a cross-architecture fashion (the same as the one used to generate

the results above) and another trained solely with x86-64 examples.

The results from these experiments are in Table 7. Both of our model variants out-perform the baseline approaches across both of the reported search pool sizes of 100 and 10000. Our KYN-Cross model performs the strongest within the 100 search pool size with a relative percentage increase of 23.4% R@1 and 12.2% MRR@10 when compared against jTrans and a relative percentage increase of 6.1% R@1 and 2.6% MRR@10 when compared against HermesSim. The difference in performance increases significantly when looking at the large search pool size of 10,000. Both model variants significantly outperform both of the benchmark approaches with the relative percentage increases of 53.95% (KYN-Cross) / 55.29% (KYN-x8664) R@1 and 46.25% (KYN-Cross) / 44.97% (KYN-x8664) MRR@10 when compared against jTrans. When compared against HermesSim, the performance increase is less but still significant with a relative percentage increase of 12.66% (KYN-Cross) / 14.11% (KYN-x8664) R@1 and 9.26% (KYN-Cross) / 7.92% (KYN-x8664).

	Cisco D1 - XC	
	100	10000
jTrans	65.0/73.8	31.4/37.4
HermesSim	75.6/80.7	48.1/54.6
KYN-Cross	80.2/82.8	54.6/59.9
KYN-x8664	77.2/80.4	55.4/59.1

Table 7: x86-64 Mono-Architecture results on Cisco Dataset-1. Results are presented with R@1 first and then MRR@10.

To further evaluate our model and understand its performance when faced with a larger x86-64 dataset, we also evaluated it against BinaryCorp-3M with and without duplicates. These results can be seen in Table 8 and show that both model variants perform similarly with the cross-architecture variant typically edging ahead. There are several areas of note. Firstly, the performance of the models when faced with a different mono-architecture dataset is significantly degraded. This highlights the need to evaluate against a range of different dataset to get a true understanding of a models performance. Secondly, the performance is inflated significantly when duplicates are present across both search pool sizes tested. This suggests that the inclusion of duplicates within evaluation datasets is a critical mistake and may lead to misrepresentation of the quality and performance of approaches.

The evaluation results show that the two KYN model variants (KYN-Cross and KYN-x8664) outperform the baseline jTrans and HermesSim approaches across different search pool sizes for the mono-architecture setting, with relative performance increases ranging from a few percent to over 50% depending on the metric and search pool size. Additionally,

	BinaryCorp3M-WD		BinaryCorp3M-ND	
	100	10000	100	10000
KYN-Cross	68.0/73.9	38.8/44.1	51.6/58.8	31.2/36.9
KYN-x86-64	67.0/73.6	36.6/41.9	51.8/58.0	31.4/36.2

Table 8: Mono-Architecture Binary Function Search Results. WD denotes "with duplicates" whilst ND denotes "no duplicates"

the presence of duplicates in the evaluation datasets is shown to significantly inflate the performance metrics, suggesting that including duplicates can misrepresent the true quality and performance of the approaches.

4.6 Cross-Architecture Binary Function Search with Inlining (RQ3)

The following section evaluates KYN in the presence of the potential of function inlining. Function inlining introduces the possibility for callee functions to be merged into (or inlined) into a caller function. If this occurs, the structure of the caller function can change significantly. This is an area which is typically highlighted as a limitation of approaches or something that is explicitly turned off [15, 19]. We chose instead of tackle this area head-on and evaluate our approach against a *BinKit* variant called *BinKit-Normal*. Within this dataset, all of the binaries have been compiled where there is a possibility for function inlining. The results presented below in Table 10 show the metric value for a given search pool size as well as the percentage difference when compared against the results present for *BinKitNoInline* in Table 6.

SP	R@1	↓	MRR@10	↓	NDCG@10	↓
100	0.73	11.6%	0.79	9.3%	0.82	8.17%
250	0.66	14.99%	0.72	13.36%	0.75	12.47%
1000	0.59	7.39%	0.66	7.42%	0.69	7.86%
10000	0.33	23.39%	0.42	20.23%	0.47	18.47%

Table 10: Binkit-Normal Metrics Across Different Search Pools with comparison against Binkit-NoInline. The percentages represent percentage decrease when function inlining was present.

The key observations from the results are as follows. Across all search pool sizes, there is a performance degradation of between 7% to 23.5% or in other works between 0.07 and 0.1 in absolute terms across the reported metrics. These results do show that function inlining does have a negative impact on our methods performance but is not dramatic. Considering that our approach was trained with a dataset that does not include function inlining, the results show our model

	ARM32	Mean Rank	Median Rank	MIPS32	Mean Rank	Median Rank
ARM32	1, 1, 1, 1	1	1	68, 14, 85, 182, 4, 44	66	56
MIPS32	8, 8, 347, 1	91	8	2, 2, 301, 12, 1, 1	53	2
X86-64	1, 1, 1, 1	1	1	79, 14, 125, 119, 6, 72	69	75.5
X86-32	1, 1, 1, 1	1	1	74, 14, 55, 144, 22, 33	57	44
RISCV-32	1, 1, 1, 326	82	1	106, 17, 34, 59, 3, 17	39	25.5
PowerPC32	967, 192, 76, 2	309	134	491, 467, 583, 63, 991, 3	433	479

Table 9: Zero Shot Vulnerability Search Results

has learnt general representation allowing it to maintain reasonable performance when faced with function inlining.

4.7 Zero-Shot Cross-Architecture Vulnerability Search (RQ4)

We also conduct a zero-shot experiment using the same methodology as the N-day vulnerability search task described in [15] but compile the same *libcrypto.so* library for RISC-V and PowerPC 32-bit to evaluate our approaches model within a zero-shot context with the results reported in Table 9.

The performance within a zero-shot context area mixed depending on the architecture used for search pool functions (i.e the architecture of what is being searched). Focusing on the ARM32 firmware image, KYN demonstrates high accuracy and precision in identifying OpenSSL vulnerabilities when provided with ARM32, x86-64, and x86-32 query functions, evidenced by a mean rank of 1 and median rank of 1. However, when faced with a MIPS32 query function, the model’s performance degrades, with a mean rank of 91 and a median rank of 8. Regarding zero-shot architectures, the RISCV-32 performance is acceptable, with a mean rank of 82 and a median rank of 1, albeit skewed by a single poor retrieval. Conversely, the PowerPC results are significantly worse, with a mean rank of 309, a median rank of 134, and a particularly high ranking of 967, indicating high variance in the model’s performance depending on the function encountered.

In addition to the ARM32 firmware image, we also report the results for the MIPS32 image within the same dataset. This is something that other works have typically omitted. Examining the MIPS32 architecture firmware, the results with a MIPS32 query function are satisfactory but inferior to the ARM32 vs. ARM32 results, with a mean score of 53 and a median of 2. When considering the in-domain architectures of ARM32, X86-64, and X86-32, the model performs acceptably, with mean ranks ranging from 57-69 and median ranks from 44-75.5, albeit not as well as the ARM32 vs. In-Domain experiments. Notably, for the out-of-domain RISCV-32 architecture, the mean and median ranks outperform all in-domain architectures. However, consistent with the ARM32 results, PowerPC32 performs poorly, with a mean rank of 433 and a

median rank of 479.

The results are mixed but show promise when compared against those reported within [4], especially for zero-shot performance of RISCV-32 \rightarrow ARM32. Our findings are however consistent with [4] in terms of MIPS32 being inherently more difficult and challenging than other architectures. The reasons for this are unclear and may warrant additional research.

4.8 Ablation Study (RQ5)

In order to understand the performance of our model in more detail and the impact of our design decisions, we trained several models on the same dataset and then evaluated them on the same test set, utilizing a search pool of 100 for evaluation to generate empirical evidence. *KYN* is the model architecture used within the rest of the paper above, *KYN-NE* is the same model architecture but the input graphs have no edge weights and therefore the edge support for *GraphConv* layers was not used and *KYN-NES* further amended whereby we replace the softmax aggregation function for add within each of the convolutional layers. The results for each of these settings can be seen below in Table 11.

Setting	MRR@10	R@1
KYN	0.80	0.76
KYN-NE	0.76	0.71
KYN-NES	0.75	0.7

Table 11: Metric scores across search pools of size 100

The results demonstrate that both the softmax aggregation and edge features contribute to increasing performance. The softmax aggregation provides a modest performance absolute improvement of 0.01 for both MRR@10 and R@1. The edge feature information however contributes to a significant absolute improvement of 0.04 MRR@10 and 0.05 of R@1. These results suggest that incorporating edge weights, in our case edge betweenness, increases the quality of the function representations for graph neural network based binary code similarity detection tasks.

During the experimentation and model development for this study, several experiments were run to understand the usefulness of various types of graph normalization techniques. Namely Layer Normalization [1], *GraphNorm* Normalization [3] and Instance Normalization [22]. To understand the effect of each, we trained the same model with the same train and test set but changed the normalization technique used within each of the 3 GNN layers.

	MRR@10	R@1
KYN + GraphNorm	0.52	0.46
KYN + LayerNorm	0.63	0.57
KYN + InstanceNorm	0.80	0.76

Table 12: Metric cross across Normalization Choices

The results presented for the normalization experiments in Table 12 are clear. They suggest that, for our data at least, the chosen normalization approach has a profound impact of the overall performance. When comparing GraphNorm to Instance Normalization, the impact of choosing GraphNorm over Instance Normalization is approximately a 0.3 absolute difference or a 42% relative difference. The effects are marginally less for LayerNorm but still significant with approximately a 0.17 absolute difference or 25% relative difference when compared against InstanceNorm.

The reason for this large performance difference likely lies within the large variations, in particular with the number of instructions within our chosen coarse node feature vectors and how both LayerNorm and GraphNorm apply normalization. Both of these normalization approaches seek to learn a normalization function for batches of graphs. Given that each of our batches contain graphs sampled from across both architectures and software projects, the variation within the batches is likely to be high. During training, the normalization functions are trained and this variation is normalized as expected. When moving to test however, when the model is faced with new software projects whereby the call graphlets have a completely different set of nodes and therefore distribution, when the learnt normalization function is applied, the normalization performs poorly. This is especially true when you look at the binaries contained within the train and test sets of the *Dataset-1* where the model is initially faced with several modestly sized projects during training before then being faced with a test dataset dominated by a very large and complex project (z3). This issue however does not effect InstanceNorm because the normalization is applied to each graph independently within a batch.

5 Limitations

Despite the promising results achieved by the KYN approach, there are several limitations that warrant further investigation.

One potential limitation lies in the computational requirements associated with generating the call graphlet representations. As the size and complexity of the target binaries increase, the computational overhead involved in extracting call graphs and constructing the graphlet neighborhoods may become prohibitive, especially in resource-constrained environments or time-sensitive applications. Future work could explore more efficient techniques for graph extraction and representation.

Another limitation of the current approach is its reliance on accurate disassembly and call graph recovery. While the methodology employed in this work assumes reliable disassembly and call graph extraction, real-world scenarios may involve obfuscated or heavily optimized binaries, which could impede accurate recovery of these structures. Techniques such as control flow flattening, virtualization obfuscation, or extreme inlining could potentially undermine the effectiveness of the proposed approach. To address this limitation, future research could investigate incorporating deobfuscation strategies or developing more robust graph recovery mechanisms that can handle adversarial obfuscation techniques.

Furthermore, the current evaluation framework primarily focuses on open-source software and benchmark datasets. While these datasets provide a valuable foundation for assessing the approach’s performance, they may not fully capture the diversity and complexity present in real-world binary analysis scenarios, such as those encountered in embedded software reverse engineering or malware analysis settings. Future work should aim to expand the evaluation scope by incorporating a broader range of proprietary software, firmware, and malware samples to further validate the approach’s generalizability and robustness under diverse and potentially adversarial conditions.

6 Conclusions

In this work, we proposed a novel graph neural network architecture called KYN that leverages one-hop call graphlets for effective cross-architecture binary function similarity detection. Our approach demonstrated state-of-the-art performance across multiple evaluation tasks spanning several benchmark datasets, consistently outperforming previous methods in both cross-architecture and mono-architecture settings. Furthermore, KYN exhibited promising results even in challenging scenarios involving function inlining and zero-shot vulnerability search across unseen architectures. Through ablation studies, we highlighted the importance of incorporating edge features and leveraging instance normalization in our model design. Overall, the proposed KYN approach provides a robust, zero-shot capable and generalizable solution for binary code similarity detection, with potential applications in areas such as N-day vulnerability detection, software forensics and malware analysis. Future research directions include extending the approach to handle advanced obfuscation techniques

and exploring its applicability to other domains within the binary analysis landscape.

Acknowledgments

I would like to acknowledge the significant contribution of the authors of [15] who have provided a foundation for robust comparison within this domain and stimulated significant research interest.

Availability

All components of this paper are publicly available. The training dataset, model training and evaluation code as well as the model artifacts themselves can be found <http://repository-to-be-made>. The tool used to generate the dataset is also open source and can be found here <https://github.com/br0kej/bin2ml>.

References

- [1] Jimmy Lei Ba, Jamie Ryan Kiros, and Geoffrey E Hinton. Layer normalization. *arXiv preprint arXiv:1607.06450*, 2016.
- [2] Tristan Benoit, Jean-Yves Marion, and Sébastien Bardin. Scalable program clone search through spectral analysis. *arXiv preprint arXiv:2210.13063*, 2022.
- [3] Tianle Cai, Shengjie Luo, Keyulu Xu, Di He, Tie-yan Liu, and Liwei Wang. Graphnorm: A principled approach to accelerating graph neural network training. In *International Conference on Machine Learning*, pages 1204–1215. PMLR, 2021.
- [4] Josh Collyer, Tim Watson, and Iain Phillips. Faser: Binary code similarity search through the use of intermediate representations. *arXiv preprint arXiv:2310.03605*, 2023.
- [5] Matthias Fey and Jan E. Lenssen. Fast graph representation learning with PyTorch Geometric. In *ICLR Workshop on Representation Learning on Graphs and Manifolds*, 2019.
- [6] Jian Gao, Yu Jiang, Zhe Liu, Xin Yang, Cong Wang, Xun Jiao, Zijiang Yang, and Jiaguang Sun. Semantic learning and emulation based cross-platform binary vulnerability seeker. *IEEE Transactions on Software Engineering*, 47(11):2575–2589, 2019.
- [7] Aric Hagberg, Pieter Swart, and Daniel S Chult. Exploring network structure, dynamics, and function using networkx. Technical report, Los Alamos National Lab.(LANL), Los Alamos, NM (United States), 2008.
- [8] Haojie He, Xingwei Lin, Ziang Weng, Ruijie Zhao, Shuitao Gan, Libo Chen, Yuede Ji, Jiashui Wang, and Zhi Xue. Code is not natural language: Unlock the power of semantics-oriented graph representation for binary code similarity detection. In *33rd USENIX Security Symposium (USENIX Security 24)*, PHILADELPHIA, PA, 2024.
- [9] Alexander Hermans, Lucas Beyer, and Bastian Leibe. In defense of the triplet loss for person re-identification. *arXiv preprint arXiv:1703.07737*, 2017.
- [10] Dongkwan Kim, Eunsoo Kim, Sang Kil Cha, Sooel Son, and Yongdae Kim. Revisiting binary code similarity analysis using interpretable feature engineering and lessons learned. *IEEE Transactions on Software Engineering*, 49(4):1661–1682, 2022.
- [11] Geunwoo Kim, Sanghyun Hong, Michael Franz, and Dokyung Song. Improving cross-platform binary analysis using representation learning via graph alignment. In *Proceedings of the 31st ACM SIGSOFT International Symposium on Software Testing and Analysis*, pages 151–163, 2022.
- [12] Diederik P Kingma and Jimmy Ba. Adam: A method for stochastic optimization. *arXiv preprint arXiv:1412.6980*, 2014.
- [13] Xuezixiang Li, Yu Qu, and Heng Yin. Palmtree: Learning an assembly language model for instruction embedding. In *Proceedings of the 2021 ACM SIGSAC Conference on Computer and Communications Security*, pages 3236–3251, 2021.
- [14] Yujia Li, Chenjie Gu, Thomas Dullien, Oriol Vinyals, and Pushmeet Kohli. Graph matching networks for learning the similarity of graph structured objects. In *International conference on machine learning*, pages 3835–3845. PMLR, 2019.
- [15] Andrea Marcelli, Mariano Graziano, Xabier Ugarte-Pedrero, Yanick Fratantonio, Mohamad Mansouri, and Davide Balzarotti. How machine learning is solving the binary function similarity problem. In *31st USENIX Security Symposium (USENIX Security 22)*, pages 2099–2116, 2022.
- [16] Christopher Morris, Martin Ritzert, Matthias Fey, William L Hamilton, Jan Eric Lenssen, Gaurav Rattan, and Martin Grohe. Weisfeiler and leman go neural: Higher-order graph neural networks. In *Proceedings of the AAAI conference on artificial intelligence*, volume 33, pages 4602–4609, 2019.
- [17] Zulie Pan, Taiyan Wang, Lu Yu, and Yintong Yan. Position distribution matters: A graph-based binary function

similarity analysis method. *Electronics*, 11(15):2446, 2022.

- [18] Kexin Pei, Zhou Xuan, Junfeng Yang, Suman Jana, and Baishakhi Ray. Trex: Learning execution semantics from micro-traces for binary similarity. *arXiv preprint arXiv:2012.08680*, 2020.
- [19] Abdullah Qasem, Mourad Debbabi, Bernard Lebel, and Marthe Kassouf. Binary function clone search in the presence of code obfuscation and optimization over multi-cpu architectures. In *Proceedings of the 2023 ACM Asia Conference on Computer and Communications Security*, pages 443–456, 2023.
- [20] Runjin Sun, Shize Guo, Jinhong Guo, Wei Li, Xingyu Zhang, Xi Guo, and Zhisong Pan. Graphmoco: A graph momentum contrast model for large-scale binary function representation learning. *Neurocomputing*, 575:127273, 2024.
- [21] Yifan Sun, Changmao Cheng, Yuhan Zhang, Chi Zhang, Liang Zheng, Zhongdao Wang, and Yichen Wei. Circle loss: A unified perspective of pair similarity optimization. In *Proceedings of the IEEE/CVF conference on computer vision and pattern recognition*, pages 6398–6407, 2020.
- [22] Dmitry Ulyanov, Andrea Vedaldi, and Victor Lempitsky. Instance normalization: The missing ingredient for fast stylization. *arXiv preprint arXiv:1607.08022*, 2016.
- [23] Hao Wang, Wenjie Qu, Gilad Katz, Wenyu Zhu, Zeyu Gao, Han Qiu, Jianwei Zhuge, and Chao Zhang. Jtrans: Jump-aware transformer for binary code similarity detection. In *Proceedings of the 31st ACM SIGSOFT International Symposium on Software Testing and Analysis*, pages 1–13, 2022.
- [24] Huaijin Wang, Pingchuan Ma, Yuanyuan Yuan, Zhibo Liu, Shuai Wang, Qiyi Tang, Sen Nie, and Shi Wu. Enhancing dnn-based binary code function search with low-cost equivalence checking. *IEEE Transactions on Software Engineering*, 49(1):226–250, 2022.
- [25] Shih-Yuan Yu, Yonatan Gizachew Achamyeh, Chonghan Wang, Anton Kocheturov, Patrick Eisen, and Mohammad Abdullah Al Faruque. Cfg2vec: Hierarchical graph neural network for cross-architectural software reverse engineering. In *2023 IEEE/ACM 45th International Conference on Software Engineering: Software Engineering in Practice (ICSE-SEIP)*, pages 281–291. IEEE, 2023.